

INFRARED STUDIES OF DUST GRAINS IN INFRARED REFLECTION NEBULAE
 Y.J. Pendleton, A.G.G.M. Tielens, and M.W. Werner
 NASA Ames Research Center

Infrared reflection nebulae, regions of dust which are illuminated by nearby embedded sources, have been observed in several regions of ongoing star formation. Near infrared observations and theoretical modelling of the scattered light from infrared reflection nebulae can provide information about the dust grain properties in star forming regions. We have modelled infrared reflection nebulae as plane parallel slabs assuming isotropically scattering grains. The intensity of the reflected light is given by

$$I = I_0 \omega f(\omega) e^{-\tau_{ext}}$$

where I_0 is the incident intensity, ω is the albedo, τ_{ext} is the foreground extinction optical depth, and the function $f(\omega)$ includes the geometric factors. In the optically thick case and when ω is small, $f(\omega)$ is independent of ω and is 0.25 for angles of incident and reflected light of 30° . Thus, $I \sim \omega$. In the optically thin limit this equation reduces to the familiar

$$I = I_0 \tau_{sca} e^{-\tau_{ext}}$$

where τ_{sca} is the scattering optical depth. For the grain scattering properties (angle averaged), we use graphite and silicate grains (Draine and Lee, 1984) with a power law grain size distribution (MRN model: $0.005 \leq a \leq 0.25$ and Large grain model: $0.225 \leq a \leq 0.8 \mu m$). The former is the well known Mathis, Rumpl, and Nordsieck (1977;MRN) model which provides a good fit to the visible and UV interstellar extinction curve. Among the free parameters of the model are the stellar luminosity and effective temperature, the optical depth of the nebula, and the extinction by foreground material.

Figure 1 shows a typical result from our model. The intensity of the reflected light increases with decreasing wavelength due to the increase in the scattering cross section. At the shortest wavelengths, it decreases again due to the rapid decrease in the intensity of the incident light for the assumed cool blackbody ($T=800K$). As shown in figure 1, the MRN grain model can explain the overall near infrared brightness of a typical infrared reflection nebula. However, larger grains can also explain the observed intensity distribution.

Besides polarization, a possible discriminant of grain size is the shape of the $3.08 \mu m$ ice band which has been observed in reflection nebulae in OMC-1 (Knacke and McCorkle, 1987), OMC-2 and Cep-A (Pendleton, 1987). Our models show that for an MRN distribution, the addition of ice mantles has little effect on the scattering cross sections. In contrast, for the large grain case, the ice produces a pronounced minimum at about $2.9 \mu m$ (fig. 2a&b). Thus, if large ice grains are present in the reflection nebula, the ice band may show structure at this wavelength unless large amounts of foreground ice extinction obfuscate this.

References:

- Knacke, R. and McCorkle, S. 1987, *A. J.*, **94**, 972.
 Mathis, J., Rumpl, W., and Nordsieck, K. 1977, **217**, 425.
 Pendleton, Y. 1987, Ph.D. thesis, U. C. Santa Cruz.

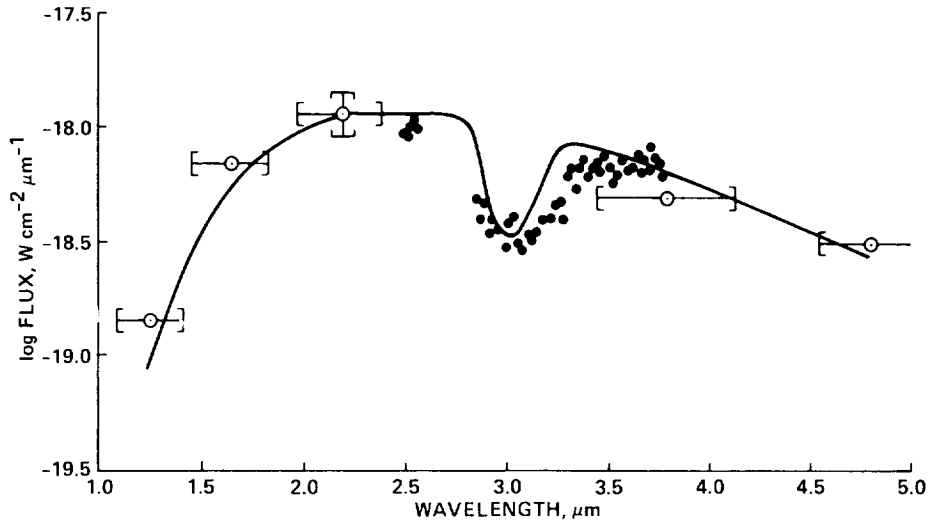


Figure 1. A comparison of model results with observations of the OMC 2 IRS1 nebula. The solid line represents isotropic scattering in an optically thick nebula over an MRN distribution of grains ($0.005 \leq a \leq 0.25 \mu\text{m}$) with 10% Oxygen in the form of ice mantles ($\Delta a_{\text{ice}} = 30 \text{ \AA}$). The broadband data for a position $5''\text{E}, 5''\text{N}$ of IRS1 are shown by open circles with brackets denoting the wavelength coverage. A typical error bar for the broadband points is shown for the $2.2 \mu\text{m}$ point. Beamsizes were $6''$ and $2.7''$ for the broadband and spectroscopic measurements, respectively. The broadband data have been multiplied by the ratio of the areas of the two beams to allow comparison to the spectroscopic data.

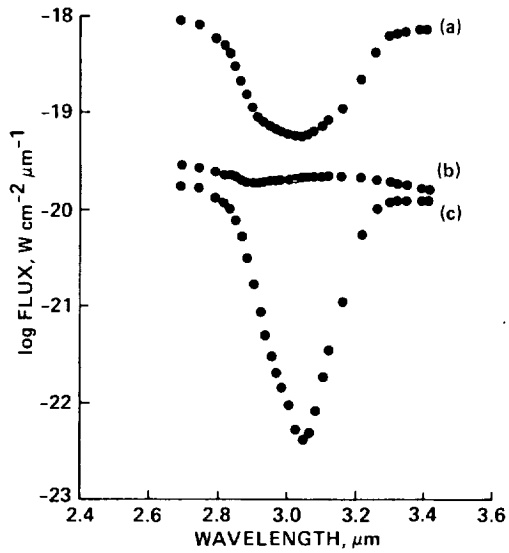


Figure 2a. A plot of flux ($\text{W cm}^{-2} \mu\text{m}^{-1}$) vs. wavelength (μm) for isotropic scattering by an MRN distribution of grains ($0.005 \leq a \leq 0.25 \mu\text{m}$) with 100% Oxygen in the form of ice mantles ($\Delta a_{\text{ice}} = 145 \text{ \AA}$). Nebular optical depth effects are shown by comparison of the optically thick curve (a) ($\sim \omega$) to the optically thin curve (b) ($\sim \tau_{\text{SCA}}$). Curve (c) demonstrates the effect of adding foreground extinction by ice particles to (b). The foreground extinction was normalized by $\tau(3.1 \mu\text{m}) = 7.0$.

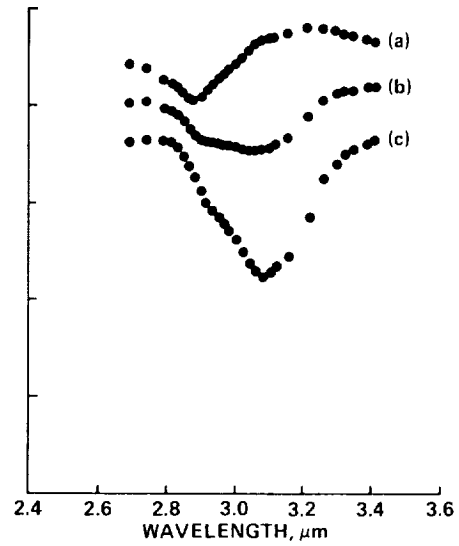


Figure 2b. A plot of flux ($\text{W cm}^{-2} \mu\text{m}^{-1}$) vs. wavelength (μm) for isotropic scattering by a distribution of large grains ($0.225 \leq a \leq 0.8 \mu\text{m}$) with 100% Oxygen in the form of ice mantles ($\Delta a_{\text{ice}} = 2600 \text{ \AA}$). In (a) we show results from an optically thick nebula while (b) and (c) represent an optically thin nebula with foreground extinction normalized such that $\tau(3.1 \mu\text{m}) = 1.5$ and 3.0 , respectively.